
Photo source: NHC, 2022

Nechako River Substrate Monitoring Program Preliminary Feasibility Assessment for a Sediment Trap and Gravel Addition at Vanderhoof, BC

Prepared by:

Northwest Hydraulic Consultants Ltd.
30 Gostick Place
North Vancouver, BC V7M 3G3
Tel: (604) 980-6011
www.nhcweb.com

NHC Project Contact:
André Zimmermann, PhD, PGeo
Principal Geomorphologist

February 22, 2023
Final Interim Report, Rev. 0

NHC Reference 3007818

Prepared for:

Ministry of Environment and Climate Change Strategy
2202 Main Mall
Vancouver, BC V6T 1Z4

Document Tracking

Date	Revision No.	Reviewer	Issued for
10-February-2023	Draft Rev. 0	S. McAdam	Client Review
22-February-2023	Final Rev. 0	S. McAdam	Project Deliverable

Report prepared by:

Unsigned report by

Simon Gauthier-Fauteux, MSc
Geomorphologist

Report reviewed by:

Unsigned report by

André Zimmermann, PhD, PGeo
Principal Geomorphologist
Senior Technical Review

DISCLAIMER

CREDITS AND ACKNOWLEDGEMENTS

The authors would like to thank the Nechako White Sturgeon Recovery Initiative and the Ministry of Environment and Climate Change Strategy for initiating this study, in particular:

- Steve McAdam — Contract Lead, Ministry of Environment and Climate Change Strategy

The following NHC personnel participated in the study:

- Barry Chilibeck — Principal-in-Charge
- André Zimmermann — Principal Geomorphologist
- Simon Gauthier-Fauteux — Geomorphologist
- Anthony Reynolds — Engineering Technologist
- Sam Chin — Technologist
- Steven Moore — Field Operations Support
- Tyler De Jong — Engineer
- Tobias Müller — Geomorphologist/Data Acquisition

NHC would also like to thank the following for their involvement in the field campaign:

- Olin Albertson — Avison Management Services Ltd.

TABLE OF CONTENTS

LIST OF TABLES IN TEXT

LIST OF FIGURES IN TEXT

1 INTRODUCTION

This document presents the results of preliminary feasibility assessments related to the excavation of a sediment trap on the Nechako River and gravel addition at Vanderhoof, BC. The purpose of this study is to evaluate the feasibility of using these approaches as restorative means to support the recovery of the endangered Nechako White Sturgeon population. Given the established link between substrate composition and white sturgeon survival (McAdam, 2011; McAdam et al., 2005), it is possible that these methods could be used, possibly in conjunction with additional treatments (e.g., substrate cleaning), to limit the amount of sand infilling spawning substrates and promote natural recruitment.

2 SEDIMENT VOLUME AND TRAP SIZE

Bedload sediment samples collected as part of previous work (NHC, 2016, 2018) were compiled and reviewed to estimate what size of sediment trap would be required to capture sand bedload upstream of a spawning pad placed in 2011 (McAdam et al., 2018; NHC, 2012). As shown on Figure 2.1, this spawning pad (referred to as the "Lower Patch") is located within the Vanderhoof reach of the Nechako River, immediately downstream of the confluence with Murray Creek. This site was selected as the most appropriate for the sediment trap feasibility analysis because it is a known spawning location, has been the focus of numerous geomorphological studies (e.g., NHC, 2012, 2014, 2016, 2018), has a large dataset including substrate mapping, bedload sediment sampling, and hydraulic modelling, and remains the focus of ongoing restoration efforts (e.g., substrate cleaning).

The following subsections describe the various components of the feasibility assessment, including the cross-channel distribution of bedload sediment transport (Section 2.1), bedload transport rating curves (Section 2.2), estimated sediment loads (Section 2.3), and estimated sizes of sediment traps required to capture sand bedload over different timeframes (Section 2.4).

Figure 2.1 Overview map of the Nechako White Sturgeon spawning reach at Vanderhoof, BC.

2.1 Cross-channel distribution of bedload sediment transport

The cross-channel distribution of bedload sediment transport was determined based on sediment sampling conducted in 2015 and 2017 (NHC, 2016, 2018). The resulting dataset has cross-channel bedload transport rates sampled across the Lower Patch on 25 days, the majority of which were collected in 2015 (NHC, 2016). The bedload transport rates were sampled throughout a wide range of flows, ranging from about 45 m^3/s to 650 m^3/s.

Consistent with previous findings (NHC, 2016, 2018), the sampling results show that the majority of the bedload sediment is conveyed within a relatively narrow portion of the channel, located approximately 20-60 m from the north bank (Table 2.1). This portion of the channel roughly corresponds to the location of the Lower Patch spawning pad, with on average 30-50% of the total sand bedload being transported approximately 30 m from the north bank at LP3, through the center of the spawning pad.

While the primary intent of this study is to assess the feasibility of a sediment trap located upstream of the Lower Patch, it may be beneficial to consider implementing a sediment trap near or at the outlet of Murray Creek (e.g., on the Murray Creek fan) given the disproportionately large amount of sediment being conveyed along the northern portion of the Nechako River (Table 2.1). The large volume of sediment being conveyed along the northern portion of the channel likely represents a mixture of both Murray Creek and Nechako River derived sediment, the relative contribution of which is not explicitly known at this time. Implementing a sediment trap at or near the outlet of Murray Creek may have a positive impact on the quality of spawning substrate located immediately downstream by limiting the tributary sediment inputs, or at a minimum may provide an indication of the relative sediment contribution from the Murray Creek system.

Table 2.1 Proportion of total bedload conveyed by each sampling location across the Lower Patch transect; contains all samples collected between 2015 and 2017.

Sampling location	Distance from north bank (m)	Proportion of total bedload (%)
LP1	10	3.5
LP2	20	9.4
LP3	30	30.2[1]
LP4	40	12.7
LP5	50	12.1
LP6	60	9.5
LP7	70	4.3
LP8	80	3.1
LP9	90	4.6
LP10	100	4.4
LP11	110	3.5
LP12	120	2.3
LP13	130	0.4

[1] There is variability in the amount of sediment transported at each site on the different sampling dates; at LP3, the proportion ranges from 0% to 99% of the total cross-sectional transport rate. The highest proportional transport rates at LP3 occurred at relatively low discharges (< 100 m^3/s).

2.2 Bedload transport rating curves

Bedload transport rates were estimated by fitting bedload-discharge rating curves to sediment samples collected in between 2013 and 2018[1] (NHC, 2014, 2015, 2016, 2018). Previous studies (Gauthier-Fauteux, 2017, 2018; NHC, 2016, 2018) have identified a complex relation between discharge and sediment transport at this location, likely related to the inverse relation between discharge and velocity caused by backwatering of the reach at high flows. Given the non-linear and weak correlation between discharge and sediment transport at this location, sediment transport rates were estimated in this study by fitting three curves to the data: an upper envelope, mean regression, and lower envelope curve (Figure 2.2). These curves were fitted by eye to generally represent the data trends, and exclude certain high and low data points.

[1] Note that the 2018 sample was collected downstream of the Burrard Ave. Bridge but is considered to be generally representative of sediment transport conditions at the Lower Patch.

The three curves were subsequently multiplied by a low flow (2014) and high flow (2015) discharge timeseries to produce upper, mean, and lower bound sediment load estimates for low flow and high flow years, as described in greater detail below (Section 2.3.1).

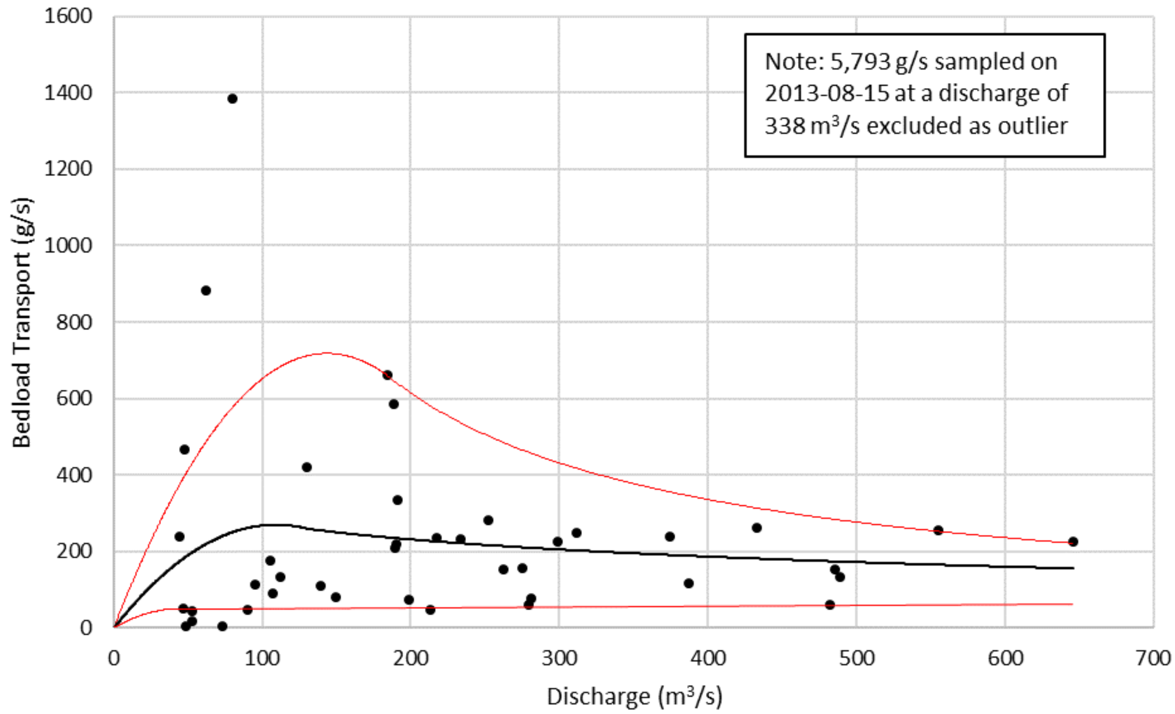

Figure 2.2 Upper bound and lower bound envelopes plotted with mean regression based on all samples collected between 2013 and 2018.

2.3 Estimated sediment loads

2.3.1 Rating curve approach

Total bedload transport across the Lower Patch transect was estimated for a low flow year (2014) and high flow year (2015) using the rating curves presented in Figure 2.2. The resulting upper bound, mean, and lower bound bedload transport estimates are plotted in relation to the low flow (2014) and high flow (2015) discharge hydrographs in Figure 2.3 and Figure 2.4, respectively. The estimated total annual sediment transport rates are tabulated in Table 2.2. The estimated bedload transport rates during two key, biologically relevant time periods, from ice-off to the end of the early rearing period (April 15 to July 7) and from the start of the spawning period to the end of the early rearing period (May 15 to July 7), are provided in Table 2.3 and Table 2.4, respectively. The bedload transport rates during these periods were estimated as they may be relevant for potential restoration planning, as further discussed in Section 2.4.

Overall, the total annual bedload transport estimates provided in Table 2.2 are in agreement with previous studies (NHC, 2016), suggesting that the total annual transport rate past the Lower Patch transect likely ranges between about 1,000 m^3/year and 8,000 m^3/year, averaging around 3,000 m^3/year to 4,000 m^3/year. The total transport rates do not show a large variation between the low flow and high flow years, which is consistent with previous studies stating that transport rates past this location tend to be relatively moderate and consistent over the course of a typical hydrograph (NHC, 2016, 2018). This may in part be explained by the relatively narrow range of shear stresses that occur at this location as a result of the inverse relation between velocity and discharge (Gauthier-Fauteux, 2017). The effects of these complex hydraulics on sediment transport can be seen on Figure 2.4, as the sediment transport rate is relatively low and constant during the peak of the 2015 hydrograph, which is in general agreement with sampling data and field observations (NHC, 2016).

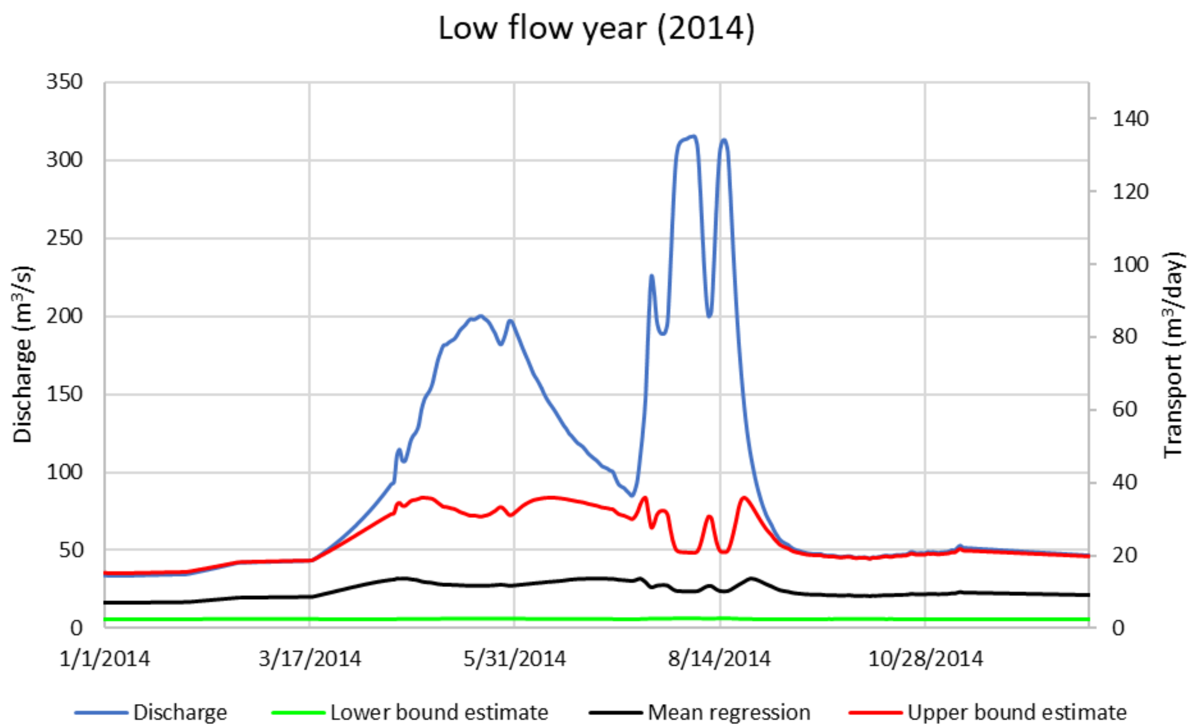

Figure 2.3 Estimated bedload transport rates during a low flow year (2014) using the rating curves presented in Figure 2.2.

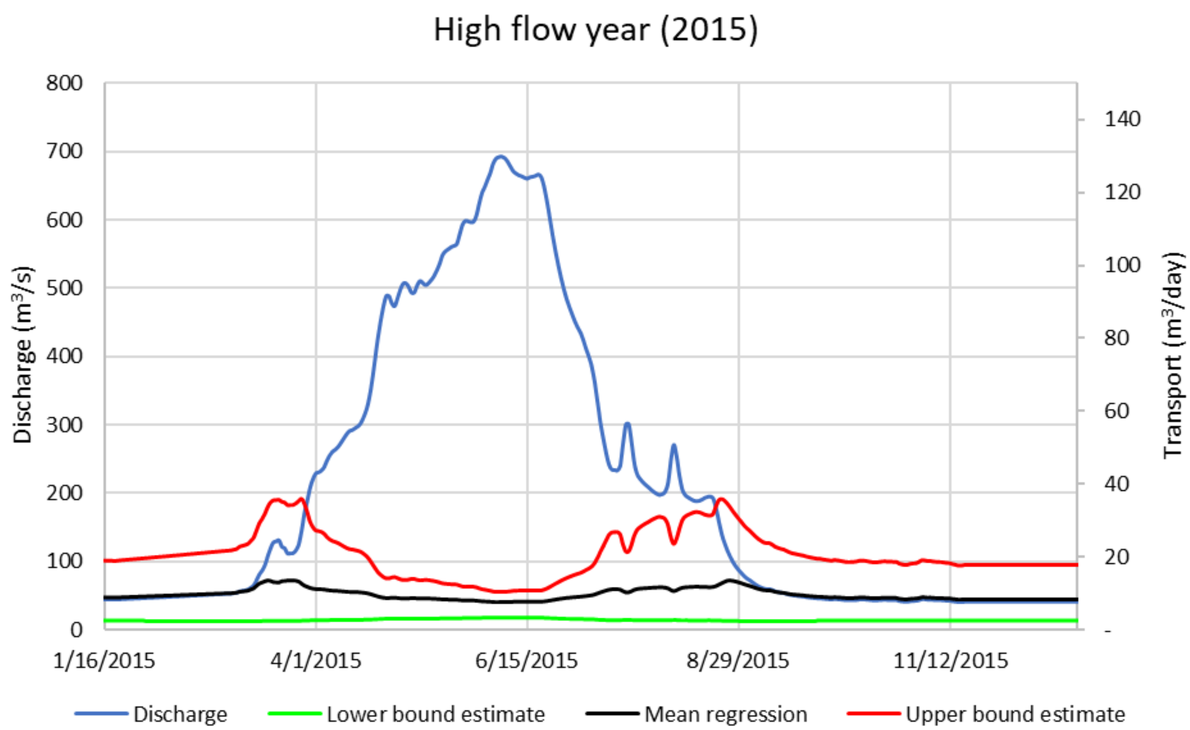

Figure 2.4 Estimated bedload transport rates for during a high flow year (2015) using the rating curves presented in Figure 2.2.

Table 2.2 Estimated annual bedload transport rates at the Lower Patch based on the rating curves presented in Figure 2.2.

Flow conditions	Annual Rates		
	Lower bound estimate (m^3)	Mean regression estimate (m^3)	Upper bound estimate (m^3)
Low flow year (2014)	903	3,744	8,819
High flow year (2015)	964	3,502	7,509

Table 2.3 Estimated bedload transport rates at the Lower Patch between ice-off and the end of the early rearing period (April 15 to July 7) based on the rating curves presented in Figure 2.2.

Flow conditions	Ice-off to end of early rearing period (April 15 to July 7)		
	Lower bound estimate (m^3)	Mean regression estimate (m^3)	Upper bound estimate (m^3)
Low flow year (2014)	212	1,055	2,835
High flow year (2015)	255	710	1,132

Table 2.4 Estimated bedload transport rates at the Lower Patch during the spawning and early rearing period (May 15 to July 7) based on the rating curves presented in Figure 2.2.

Flow conditions	Spawning and early rearing period (May 15 to July 7)		
	Lower bound estimate (m^3)	Mean regression estimate (m^3)	Upper bound estimate (m^3)
Low flow year (2014)	137	678	1,820
High flow year (2015)	168	439	661

2.3.2 Infilling of substrate grids

Data collected by substrate monitoring grids deployed in April 2022 were used as a second method to estimate bedload transport rates within the spawning reach. Details regarding the substrate grids and monitoring results are provided elsewhere (NHC, 2022), and thus only briefly described herein.

Three substrate grids were deployed immediately prior to the 2022 spawning period to continuously monitor infilling of spawning gravels at the three locations shown on Figure 2.5. Each substrate grid consisted of a 1 m x 1 m x 0.1 m steel frame that was filled with clean gravel and placed on the riverbed. A heating element along with an array of temperature sensors were embedded within the gravels to remotely monitor sediment infiltration based on the hot wire principle (Zimmermann and Lapointe, 2005), where the amount of heat removed by a fluid can be related to the fluid's velocity; thus, sedimentation within interstitial voids would reduce the intergravel flow velocity, resulting in both an increase in the magnitude and (under ideal conditions) the duration of the heat pulse transferred downstream.

The sensor arrays showed that the rate of infilling varied depending on cross-channel location; however, all sites ultimately infilled with fine sediment over time. The sensor array nearest to the center of the channel ("Offshore Sensor Array (Grid 1378)") showed that fine sediment began infilling the gravel substrate within 2 days of deployment, while the middle sensor array ("Middle Sensor Array (Grid 1379)") took 10 days, and the left bank sensor array ("Inshore Sensor Array (Grid 1377)") took 26 days for initial infilling to occur. The amount of time from when the substrate grids began to infill (i.e., first heat pulse measured by any one sensor) and at least partial infilling of the entire grid (i.e., heat pulse measured by all five sensors) for the Offshore Sensor Array (Grid 1378), Middle Sensor Array (Grid 1379), and Inshore Sensor Array (Grid 1377) was 3 days, 21 days, and 29 days, respectively.

The amount of time required for initial infilling (as detected by the sensor nearest to the heating element) and at least partial infilling of the entire grid (as detected by sensor furthest from the heating element) were used to estimated bedload transport rates at each grid location. To do so, the volume of sand required to infill the grids was estimated using the grid geometry, sensor arrangement, and porosity of the placed gravel substrate, measured in the lab to contain approximately 39% voids. The estimated bedload transport rates at each location are presented in Table 2.5.

The resulting estimates presented in Table 2.5 are considerably lower than the bedload transport estimates obtained using the rating curve approach described in Section 2.3.1. It is likely that the estimates produced using the substrate monitoring grids underestimate the actual transport rate over natural substrate because the steel frames were deployed proud of the riverbed, likely causing some bedload to be diverted around the frames. In addition, a certain duration would likely be required for bedload sediment to accumulate at the upstream end of the frame before infilling the frame itself, thus prolonging the amount of time required for infilling to occur (i.e., infilling of natural substrates may occur even quicker than as detected by the substrate grids). Overall, these estimates are considered to provide lower-bound estimates of sediment transport, but are likely less representative of actual conditions than those produced using the rating curve approach (Table 2.2; Table 2.3; Table 2.4); thus, the sediment volumes generated using the rating curve approach were used to estimate the required trap size in Section 2.4.

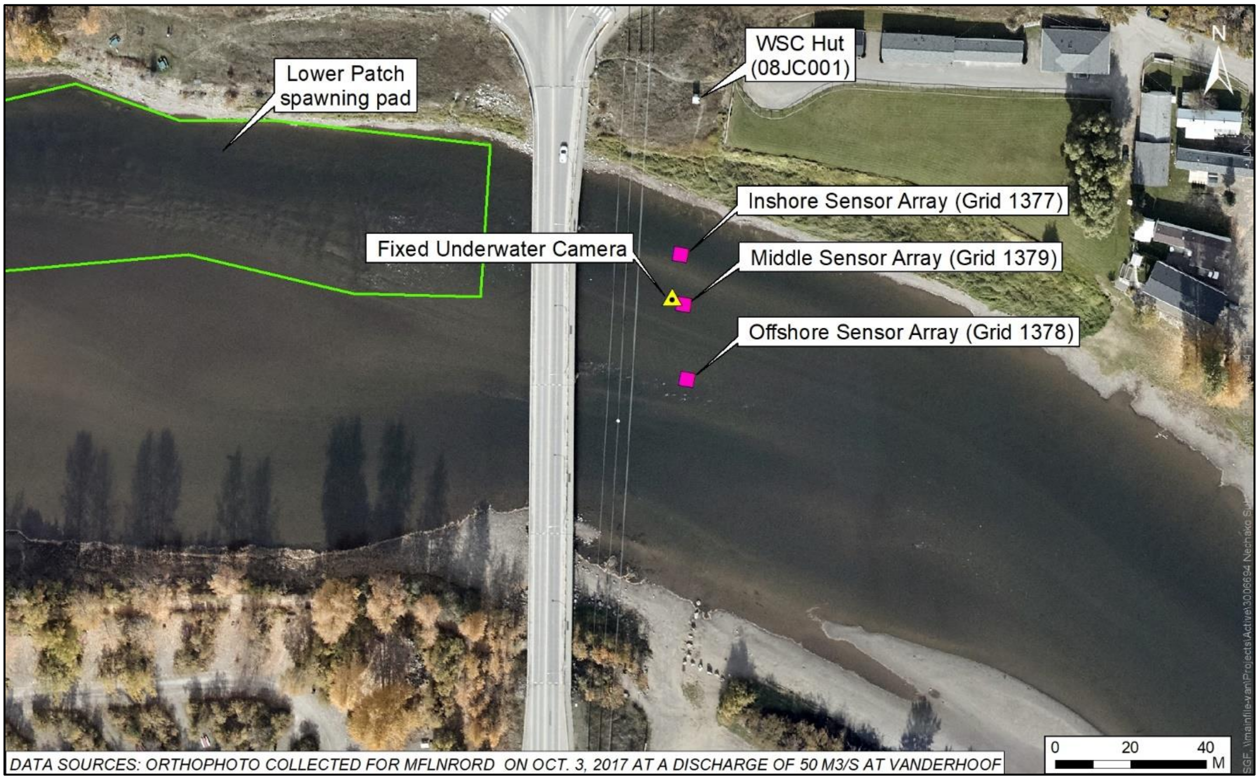

Figure 2.5 Locations where three temperature sensor arrays were deployed in April 2022 to continuously monitor infilling of spawning gravels within the spawning reach.

Table 2.5 Estimated sediment transport rates based on substrate monitoring grids.

Substrate grid	Estimated transport rate per unit width	Estimated cross-channel transport rate[1]
Grid 1377 (Inshore)	0.1-0.2 m^2/year	15-25 m^3/year
Grid 1379 (Middle)	0.3-0.4 m^2/year	42-49 m^3/year
Grid 1378 (Offshore)	1.9-2.3 m^2/year	247-293 m^3/year

[1] Based on a 130 m channel width.

2.4 Estimated size of sediment trap

To estimate what size of sediment trap would be required to capture sand bedload, the total estimated sediment transport volumes shown in Table 2.2, Table 2.3, and Table 2.4 were distributed across the channel based on proportions shown in Table 2.1. It was assumed that the sediment trap would be 2 m deep and 50 m in cross-channel length, spanning from the LP1 to LP5 sampling locations shown in Table 2.1. This cross-channel distance roughly corresponds to the width and location of the upstream extent of the Lower Patch spawning pad shown on Figure 2.1. Estimates of the total annual bedload transport rate across this portion of the channel during low flow (2014) and high flow (2015) conditions, as well as estimates of sediment transport specifically during the spawning period, are presented in Table 2.6.

Table 2.6 Estimated sediment volumes over a cross-channel distance of 50 m (LP1 to LP5) based on the rating curves presented in Figure 2.2.

Design condition	Lower bound estimate (m^3)	Mean regression estimate (m^3)	Upper bound estimate (m^3)
Annual rate – low flow (2014)	614	2,545	5,995
Annual rate – high flow (2015)	655	2,381	5,105
April 15 to July 7[1] – low flow (2014)	144	717	1,927
April 15 to July 7[1] – high flow (2015)	174	482	769
May 15 to July 7[2] – low flow (2014)	93	461	1,237
May 15 to July 7[2] – high flow (2015)	114	298	449

[1] This timeframe represents the period between ice-off and the end of the early rearing stage.
[2] This timeframe represents the spawning and early rearing period.

The sediment volumes presented above (Table 2.6) were used to estimate the trap length required to contain sediment for the various design conditions based on an assumed cross-channel trap width of 50 m (LP1 to LP5) and depth of 2 m, the results of which are presented in Table 2.7. The minimum recommended trap length for each design condition (Table 2.7) represents the minimum trap length required to contain the upper bound sediment transport estimate at the LP3 sampling site, which conveys a disproportionately large amount of bedload sediment (Table 2.1). This was done because if the trap is of insufficient length to contain the amount of bedload conveyed at this specific location, it is presumed that the trap would fill locally and bedload would be conveyed overtop (i.e., the trap efficiency would be greatly reduced).

Table 2.7 Estimated trap length required to contain sediment for the various design conditions based on an assumed cross-channel trap width of 50 m (LP1 to LP5) and depth of 2 m.

Design condition	Recommended trap length (m) to contain lower bound estimate across LP1-LP5	Recommended trap length (m) to contain mean regression estimate across LP1-LP5	Recommended trap length (m) to contain upper bound estimate across LP1-LP5	Minimum recommended trap length (m) to contain upper bound estimate at LP3
Annual rate – low flow (2014)	6	25	60	27
Annual rate – high flow (2015)	7	24	51	23
April 15 to July 7[1] – low flow (2014)	1	7	19	9
April 15 to July 7[1] – high flow (2015)	2	5	8	3
May 15 to July 7[2] – low flow (2014)	1	5	12	5
May 15 to July 7[2] – high flow (2015)	1	3	4	2

The recommended trap dimensions presented above assume that the trap is cleaned out once per year. However, trap size could be decreased if maintenance were to be conducted more frequently. The resulting required trap size would depend on the maintenance schedule and rate of sediment removal, where the volumetric capacity of the trap plus the rate of sediment removal should equal or exceed the estimated volumes present in Table 2.6.

It is also important to note the inherent uncertainty in estimating bedload transport rates, which in turn creates uncertainty in estimating the required trap dimensions. The values presented above should be interpreted with an appropriate degree of uncertainty, where the dimensions could vary by a factor of two, likely up to a factor of ten.

3 GRAINSIZE MOBILITY FOR GRAVEL ADDITION

The second component of this study was to complete a preliminary assessment of grainsize mobility to inform the design and expected function of gravel addition within the spawning reach. Grainsize mobility was primarily assessed based on the large bedload sampling dataset collected during previous studies (NHC, 2016, 2018), and supplemented by sediment transport calculations using simulated hydraulics (Gauthier-Fauteux, 2017, 2018). The resulting grainsize mobility estimates are further described below.

The dataset used to inform grainsize mobility included cross-channel bedload samples collected on 13 days in 2015 and 2017 (NHC, 2016, 2018), during which the discharge at Vanderhoof ranged from about

45 m^3/s to 650 m^3/s. Each these samples were sieved as part of previous work (Gauthier-Fauteux, 2017; NHC, 2016, 2018), allowing for the mixture of bedload sediment to be segmented by size class. Figure 3.1 plots the maximum sampled grainsize (i.e., largest mobile grainsize collected by the sampler) on each sampling date against the discharge at Vanderhoof when the sample was collected.

As shown on the plot below, the maximum mobile grainsize sampled across the Lower Patch sampling transect was 16 mm, which occurred during both low flow (105 m^3/s and 140 m^3/s) and high flow (660 m^3/s) conditions. No strong positive correlation exists between discharge and mobile grainsize at this location, likely due to the relatively narrow range of shear stresses that occur as a result of the inverse relation between velocity and discharge (Gauthier-Fauteux, 2017).

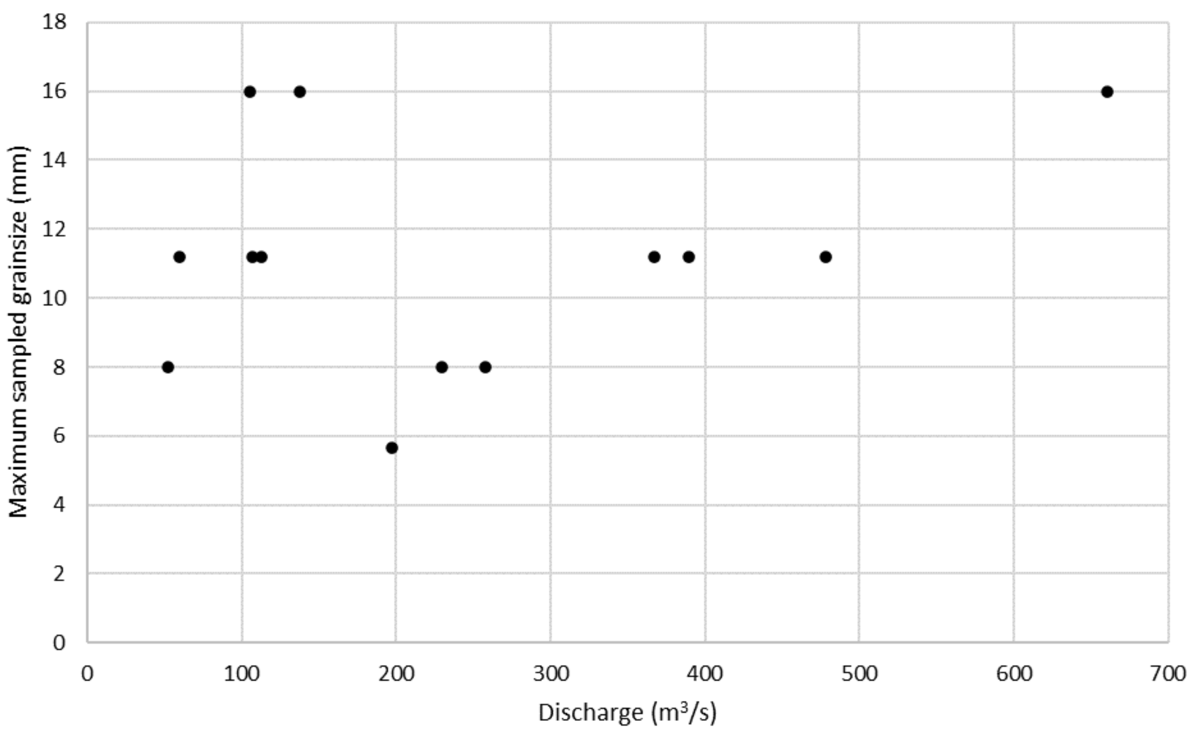

Figure 3.1 Maximum sampled grainsize plotted against discharge at Vanderhoof; dataset contains 10 sieved bedload samples from 2015 and 3 sieved samples from 2017, all collected using a Helley-Smith sampler.

Sediment transport calculations were done to supplement the empirical estimates of grainsize mobility described above using simulated hydraulics from a 2-D (depth-averaged) numerical model (Gauthier-Fauteux, 2017, 2018). Based on the results from numerically simulated flows ranging from 75 m^3/s to 675 m^3/s, the maximum depth-averaged shear stress expected to occur around the Lower Patch is approximately 12 N/m^2. In practice some of this stress may be exerted on the channel form and bridge structure in addition to the river bed. As an upper bound, all of the stress is considered to be applied to the bed. Partitioning the depth-averaged shear stress into that exerted solely on the grains was considered beyond the scope of this preliminary assessment.

The maximum mobile grainsize was predicted based on the shear stress approach originally presented by Shields (1936) using the following equation:

$$D = \frac{\tau}{(\rho_s - \rho)\ g\ \tau_{cr}^{*}} \qquad (1)$$

Where D is the maximum mobile grainsize, τ is the maximum expected shear stress (12 N/m^2), τ_{cr}^{*} is the critical Shields parameter that was set to 0.045 to represent incipient motion for medium gravels (USGS, 2008), ρ_s and ρ are the density of sediment and water, respectively ($\rho_s = 2650\ kg/m^3$ and $\rho = 1000\ kg/m^3$), and g is the acceleration of gravity (9.81 m/s^2). By solving for D, the maximum mobile grainsize is predicted to be around 16 mm, which is in agreement with the sampled data presented in Figure 3.1.

While both approaches suggest that the maximum mobile grainsize is around 16 mm, visual observations using a fixed underwater camera (NHC, 2022) suggest that some grains in the 16-32 mm range are periodically mobilized as well, likely due to near-bed turbulent fluctuations that are not captured by the depth-averaged model. The bedload sediment samples also likely underestimate the maximum mobile grainsize due to sampler bias, which tends to have a lower probability of being collected in the sampler due to the low frequency with which they are moved and sporadic nature of gravel transport. Thus, it is likely that the maximum grainsize that can be transported downstream ranges between 16-32 mm. The actual amount of 32 mm sediment transported would be relatively small and there would be limited downstream dispersal of this sediment size.

The preliminary grainsize mobility estimates suggest that the grainsize distribution used for gravel addition would need to be relatively fine (i.e., finer than 16 mm) to have any considerable amount of downstream transport and dispersal. If a coarser grainsize distribution were to be used, for example up to 32 mm, it is likely that a proportion of the coarser grains would get periodically mobilized and displaced a short distance downstream (e.g., a few meters), but with no largescale dispersal of the material. Based on the preliminary calculations described above, the expected maximum shear stress of 12 N/m^2 would need to double to transport any appreciable amount of 32 mm gravels, which would likely require considerable alteration to the local flow hydraulics (e.g., building up a large enough sediment deposit to locally increase shear stress). If this approach is to be pursued, it is recommended that further studies be completed to determine whether 16 mm gravel can produce biologically functional habitat that supports natural recruitment and to assess changes in flood and public risk (e.g., navigational hazards) caused by the channel alterations required to locally increase shear stress and transport larger grains. Initially it is suspected that the interstitial space between 16 mm grains may not be large enough for larvae to enter; however, this would need to be confirmed.

4 REFERENCES

Gauthier-Fauteux, S. (2017). *Linking Fluvial Dynamics to White Sturgeon Habitat in the Nechako River, BC.* (M.Sc. thesis). University of British Columbia, Vancouver, BC.

Gauthier-Fauteux, S. (2018). *2018 Hydrodynamic Modelling Nechako River at Vanderhoof, BC*. Draft Report. Prepared by S. Gauthier-Fauteux for Ministry of Environment and Climate Change Strategy. 1–103 pp.

McAdam, S. O. (2011). Effects of substrate condition on habitat use and survival by white sturgeon (Acipenser transmontanus) larvae and potential implications for recruitment. *Canadian Journal of Fisheries and Aquatic Sciences*, 68(5), 812–822. doi:10.1139/f2011-021.

McAdam, S. O., Crossman, J. A., Williamson, C., St-Onge, I., Dion, R., Manny, B. A., and Gessner, J. (2018). If you build it, will they come? Spawning habitat remediation for sturgeon. *Journal of Applied Ichthyology*, 34(2), 258–278.

McAdam, S. O., Walters, C. J., and Nistor, C. J. (2005). Linkages between white sturgeon recruitment and altered bed substrates in the Nechako River, Canada. *Trans. Amer. Fish Soc.*, 134, 1448–1456.

NHC (2012). *Nechako Sturgeon Spawning Gravel September, 2011 Substrate Assessment*. Prepared by Northwest Hydraulic Consultants for Ministry of Forests, Lands and Natural Resource Operations, North Vancouver. 60 pp.

NHC (2014). *Nechako River 2013 Sediment Transport Investigations*. Prepared by Northwest Hydraulic Consultants for the Ministry of Forests, Lands and Natural Resource Operations, North Vancouver BC. 48 pp.

NHC (2015). *2014 Sediment Transport Investigation on the Vanderhoof Reach of the Nechako River*. Prepared for Ministry of Forests, Lands and Natural Resource Operations, North Vancouver. 42 pp.

NHC (2016). *2015 Sediment Transport Investigation on the Vanderhoof Reach of the Nechako River.* Final Report. Prepared for the Ministry of Forests, Lands and Natural Resource Operations by Northwest Hydraulic Consultants Ltd., North Vancouver, BC. 69 pp.

NHC (2018). *2017 Nechako River Geomorphology Report.* Draft Report. Prepared for the Ministry of Forests, Lands, Natural Resource Operations and Rural Development by Northwest Hydraulic Consultants Ltd., North Vancouver, BC. 83 pp.

NHC (2022). *Nechako River Substrate Monitoring Program: 2022 Design and Installation Report*. Final Draft. Prepared by Northwest Hydraulic Consultants for Ministry of Environment and Climate Change Strategy, North Vancouver, BC. 20 pp.

Shields, A. (1936). *Application of similarity principles and turbulence research to bed-load movement*. Mitteilungen der Preussischen Versuchsanstalt fur Wasserbau und Schiffbau.

USGS (2008). *Simulation of Flow, Sediment Transport, and Sediment Mobility of the Lower Coeur d'Alene River, Idaho* (2008–5093). Scientific Investigations Report. Prepared in cooperation with the

Idaho Department of Environmental Quality, Basin Environmental Improvement Commission, and the U.S. Environmental Protection Agency, Virginia. 164 pp.

Zimmermann, A., and Lapointe, M. (2005). Intergranular flow velocity through salmonid redds: Sensitivity to fines infiltration from low intensity sediment transport events. *Rivers Research and Applications*, 21, 865–881.